Investigation of Spatial and Temporal Trends in Lake Toba Water Level Based on ICESat-2 Data

Widyani Galih Pangersa [1*], *), Ni Made Rai Ratih Cahya Perbani[2]

[1] Undergraduate Program in Geodetic Engineering, Institut Teknologi Nasional Bandung, Indonesia

[2] Doctoral Program in Geodesy and Geomatics, Institut Teknologi Bandung

*glhpngrs@gmail.com

Abstract **:** *Lake Toba is the largest volcanic lake in Indonesia and one of the 15 lakes prioritized by the Indonesian government. As the largest volcanic lake in Southeast Asia, it serves as a critical freshwater reservoir, supports fisheries and tourism, and influences local hydrological and climatic conditions. It also plays an important role in climate change, so fluctuations in its water level need to be monitored continuously. ICESat-2 is a laser based measurement satellite equipped with the Advanced Topographic Laser Altimeter System (ATLAS), which works by counting photons and enables periodic monitoring of water levels. This study focuses on identifying spatial and temporal trends in water levels in Lake Toba using ICESat-2 ATL13 data from 2018 to 2024. The parameters analyzed were segment latitude (segmen_lat), segment longitude (segmen_long), and water surface height (ht_water_surf) from Tracks 385, 825, and 1269. Spatial analysis was conducted using profiles and 3D models along the satellite tracks across Lake Toba. Meanwhile, temporal analysis was performed using temporal data samples on tracks 285, 825, and 1269, which were bounded by the area along each respective track, by selecting data that had the most observation months. Then least square analysis was conducted for temporal modeling Based on the analysis of ICESat-2 data in Tracks 385, 825, and 1269, it was found that the water level in the eastern part of Lake Toba is higher than in the western and central parts, with differences reaching approximately 2.4 meters. A pattern of water level accumulation toward the mainland was also observed in the three-dimensional profiles. Between 2018 and 2024, the lowest water level occurred in 2021. In general, the variation in water levels was influenced by both annual (Sa) and semi-annual (Ssa) cycles, with Ssa being more dominant. These findings provide new insights into the spatial and temporal dynamics of Lake Toba water levels.*

Keywords: ICESat-2 ATL-13, Lake Toba, Spatial trend, Temporal trend, Water level

Introduction

Lake Toba is a volcanic lake formed by a mega-colossal eruption of Mount Toba that occurred 74,000 years ago. As a result of this eruption, Lake Toba has a hilly and valley topography. This uniqueness is utilized by the community for tourism activities, trade, fisheries with floating net cages (KJA), water sources for regional water companies (PDAM) (Thesalonika, 2017), and water sources for three hydroelectric power plants: Sigura-gura, Tangga, and

Hasang (Hidayat, 2020; Rini, 2022), thus, Lake Toba plays an important role in North Sumatra's economy.

However, in the past six decades, Lake Toba has experienced significant water level decline (Rosid et al., 2025). Until 2021, Lake Toba experienced drastic water level decline approaching its minimum limit with a decline rate of one centimeter per day (Budianto, 2023). This condition would certainly disrupt Lake Toba's economic wheel. Therefore, the Indonesian Government issued regulations through Presidential Regulation (PERPRES) Number 60 of 2021 concerning the Rescue of National Priority Lakes, where Lake Toba is included as one of the 15 prioritized lakes. This was done to regulate priority lake rescue efforts and provide guidelines in managing and controlling business processes and activities related to priority lake rescue.

Changes in lake water level can be caused by several factors, such as climate change which affects changes in rainfall and air temperature, as well as human activities that contribute to lake water level fluctuations (De Wit & Stankiewicz, 2006; Robertson & Ragotzkie, 1990; Rosid et al., 2025).

The use of altimetry satellites is often used in inland water research. However, conventional altimetry satellites have relatively large footprints on the earth's surface, and the size of these footprints depends on surface characteristics (from 1.65 to 20 km(Phan et al., 2012; Sichangi et al., 2016), which makes the required inland water data contaminated by lake edge topography, thus reducing measurement accuracy for small inland waters.

ICESat-2, based on photon-counting laser altimeter, was launched by NASA in 2018. ICESat-2 carries an instrument called the Advanced Topographic Laser Altimeter System (ATLAS) that transmits 10,000 pulses per second, 250 times faster than ICESat-1. Each laser beam has a footprint diameter of 17 m with a sampling interval along the track of 0.7 m (Liu et al., 2022). With ICESat-2's capabilities, the topographic characteristics of Lake Toba, which has Samosir Island in its center, becomes a challenge that can be overcome by providing higher resolution. Furthermore, ICESat-2 collects data through a multi-histogram altitude zones (multi-Haz) photon counting system that is sensitive at the single photon level, greatly improving data coverage density and data accuracy (Fernando & Pedro, 2023).

This research uses water level data from ICESat-2 from 2018 to 2024. ICESat-2 has advantages in high spatial resolution and has proven effective in monitoring water bodies such as lakes. This data is then analyzed to investigate spatial and temporal trends in water levels at Lake Toba, so it can be used to assess the dynamics of lake water levels over the long term and monitor threats of water level decline to support the rescue of Lake Toba as a National Priority Lake, as well as periodic flood disasters.

Literature Review

ICESat-2 with ATL-13 data products focuses on collecting information for water bodies such as lakes in inland waters. ICESat-2 ATL13 measures inland waters defined as adjacent continental water bodies, including lakes and reservoirs with areas greater than 0.1 km^2, rivers with widths of 50-100 meters, transitional waters such as estuaries and bays, and coastal areas up to 7 km from the coastline (Jasinski et al., 2023). ICESat-2 assumes water level height in inland waters with Gaussian distribution as a practical approach. This assumption is considered suitable for lakes or small water bodies (<5 km to 50 km) because their fetch and wave heights are small, so the distribution is closer to normal (Jasinski et al., 2023)

Previous research using ICESat-2 conducted by Xiang et al (2021). stated that ICESat-2 has better accuracy compared to ICESat-1 and GEDI with RMSE results of 0.06 m for lakes and 0.012 m for rivers. Research by Liu et al. (2022) also showed that comparison of ICESat-2 data and in situ data for water height produces linear regression with strong relationships. When in situ data datum is adjusted to ICESat-2 datum, the RMSE of both produces seven cm. The use of ATL-13 in estimating lake water level has also been successfully done by Fernando & Pedro (2023) at Lake Yahuarcocha with results showing that water level estimated from ATL13 is the same as the trend of water level measured on site, with an average estimation error of 30 cm. This figure is considered small, so it can be concluded that ICESat-2 ATL-13 data has a high level of precision.

From these various studies, it can be concluded that ICESat-2, particularly the ATL-13 product, has reliable capabilities in monitoring small inland waters with high precision levels. However, until now its utilization for water level analysis in Indonesia has not been widely conducted. Therefore, this research focuses on the application of ICESat-2 ATL-13 data to assess water level dynamics in Indonesian waters, with a case study at Lake Toba

Methodology

The research was conducted on Lake Toba, North Sumatra Province. Geographically, Lake Toba is located between 2°21'32" to 2°56'28" N and 98°26'35" to 99°15'40" E. The lake, with a surface area of approximately 1,124 km² and a land area (lake catchment area) of approximately 2,486 km², is surrounded by four main watershed groups: the Barisan Mountain Range, Barisan Foothills, Toba Plateau, and Toba Depression. The watershed area that drains into Lake Toba originates from rainfall and water from rivers flowing into the lake. Around the lake, there are 19 major sub-watersheds from 19 rivers flowing into Lake Toba (Lukman, 2013). According to Meigh (1990), there are 295 rivers flowing into Lake Toba. Most of these rivers have relatively small watersheds with an average area of 8.2 km², with only a few having watersheds larger than 100 km². In this research, ICESat-2 will be used to demonstrate its ability to read water levels and subsequently observe their spatial and temporal trends.

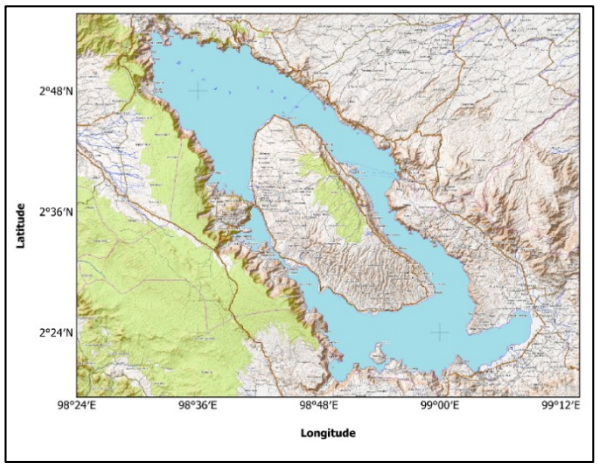

Source: Basemap OpenTopoMap

Figure 1: Studi Area of Toba Lake

This research was conducted in several stages, including the ATL13 data download, selection of relevant parameters (latitude, longitude, and water level), and sampling of these parameters to obtain latitude, longitude, and water level data for each track. This data will be used to create scatter plots and 3D modeling for spatial trend analysis and harmonic analysis to determine the possibility of periodic behavior. The research methodology flowchart is shown in the Figure 2.

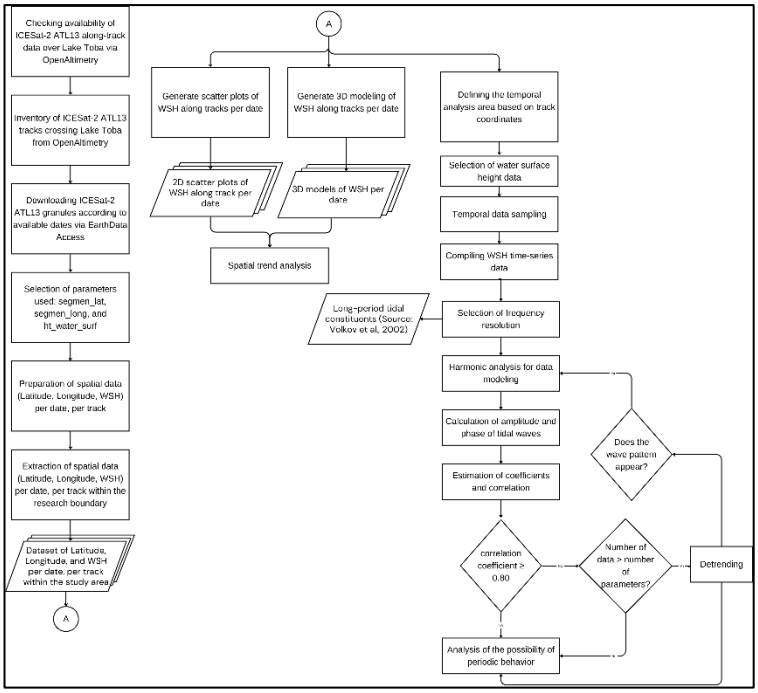

Souce: Personal Documentation

Figure 2: Flowchart of methodology

The data range used in this study spans from 2018 to 2024. ICESat-2 has a temporal resolution of 91 days, so ideally, ICESat-2 will pass over Lake Toba again every three months. ICESat-2 orbits through Lake Toba with 5 available tracks: 73, 385, 825, 1017, and 1269. Three tracks (385, 825, and 1269) are used in this study, as they can represent different regions of Lake Toba: the eastern part is represented by track 1269, the western part by track 385, and the central part by track 825. The orbital routes and datasets available on ICESat-2 can be accessed through https://openaltimetry.earthdatacloud.nasa.gov/. To determine available dataset dates, users should select the available track lines on the orbital route."

Dataset downloads can be performed through Earth Data Search (https://search.earthdata.nasa.gov/) by matching the track ID and time available on Open Altimetry. Downloaded data will be in HDF5 format containing track data with gt1-gt3 tracks, each having left and right beam pairs. The data to be used in research processing are the segment_lat, segment_long, and ht_water_surface datasets.

The downloaded data originates from one Earth orbit, so data sampling steps are necessary to separate the data used in the research. Data sampling is performed by building a Python script that limits data extraction using minimum and maximum values from each latitude and longitude of respective tracks, followed by combining data from tracks gt1-gt3. The result of data sampling is latitude, longitude, and water surface height per track per date,

saved in CSV forma

Each data sampling result is then visualized as scatter plots for further spatial analysis, requiring uniform scale bar legends for comparison purposes. Scatter plot creation uses Python scripts. Additionally, the data is also processed into three-dimensional models using Surfer to help understand water surface height dynamics in detail through integration of length, width, and height of the data. These scatter plots and 3D modeling will be used in spatial analysis.

For temporal analysis, the data to be used needs to be sorted again. The data criteria are: a) having consistent occurrence data; b) data are in the same or nearby latitude/longitude areas. Therefore, data sampling results need to be sampled first. Data sampling in this study is performed by building a Python script to define grid areas based on minimum and maximum limits of latitude and longitude values on each track as the main area, which is then divided into 17 meter × 17 meter grid sizes where each data point will be mapped to the grid corresponding to the grid center coordinates. If more than one data point falls within a grid size, the data will be averaged, so each grid will only have one latitude, longitude, and water surface height value. Grids without ICESat-2 data will be filled with a value of 9999. The sampling approach follows ICESat-2's spatial resolution of a 17-meter footprint. Next, data filtering is performed by removing 9999 values to obtain filtered data per track as shown in example of data filtering from Track 825 Table 1.

Table 1: Data filtering result for Track 825

Latitude (°)	**Longitude (°)**	**Height (m)**	**Latitude (DMS)**	**Longitude (DMS)**
2,44023	98,79609	892,4767	2° 26' 24,83"	98° 47' 45,92"
2,44038	98,79609	892,4352	2° 26' 25,37"	98° 47' 45,92"
2,44053	98,79609	892,4635	2° 26' 25,91"	98° 47' 45,92"
⋮	⋮	⋮	⋮	⋮
2,80094	98,78036	891,2232767	2° 48' 3,38"	98° 46' 49,30"
2,80109	98,78036	891,21798	2° 48' 3,92"	98° 46' 49,30"
2,80124	98,78036	891,225435	2° 48' 4,46"	98° 46' 49,30"

The filtered data is then sorted again based on criteria of being at the same location (latitude) but at different times. Data selection is assisted by building a Python script, and the resulting

water surface heights are then saved in CSV format. Table 2 shows selected data for water surface height on each track.

Table 2: Selected Data for Water Surface Height on Each Track

Track	Latitude	Longitude	Height	Date
385	2.86487	98.58490	890.06340	23/10/2018
	2.86487	98.58581	890.24070	20/04/2020
	2.86487	98.58276	890.05720	19/10/2020
	2.86487	98.64720	890.46858	19/04/2021
	2.86487	98.57909	890.80994	17/04/2022
	2.86487	98.58597	890.62053	17/07/2022
	2.86487	98.55038	890.59980	15/04/2023
	2.86487	98.54657	890.42566	15/07/2023
	2.86487	98.57955	890.91470	12/07/2024
825	2.76016	98.80235	891.94336	20/02/2019
	2.76016	98.82770	891.73236	18/02/2020
	2.76016	98.67255	890.63618	16/02/2021
	2.76016	98.79853	891.56433	14/02/2022
	2.76016	98.81854	891.97590	14/05/2023
	2.76016	98.75394	891.47460	12/11/2023
1269	2.76016	98.77624	891.14572	21/11/2018
	2.38348	98.99919	893.14276	20/12/2018
	2.38348	99.01431	893.28156	21/03/2019
	2.38348	99.02073	892.68868	19/09/2019
	2.38348	99.02149	892.74090	18/03/2020
	2.38348	98.95918	892.45100	16/09/2020
	2.38348	98.89459	892.16133	17/03/2021
	2.38348	99.13419	894.09950	14/06/2022
	2.38348	98.98820	892.94916	11/09/2023
	2.38348	98.97568	893.34511	11/12/2023
	2.38348	98.92711	893.17690	10/03/2024

To understand the periodic patterns of water surface height fluctuations, harmonic analysis is performed to decompose tidal signals into main components based on their harmonic constants. Harmonic analysis is conducted through several stages. The initial stage is converting the date format from DDMMYYYY to Julian Date to standardize the time format for use in subsequent calculations.

Next, tidal data compilation is performed consisting of water surface height (h), time in Julian Date format (t), and angular velocity values (ω). The tidal constants selected for angular velocity in the analysis are constants that meet certain frequency limitations. In this

study, Sa and Ssa are used as they meet the frequency limitations of each available track.

The next stage is matrix compilation by forming a design matrix (A) based on angular velocity values (ω) from selected constants.

$$[\mathrm{A}] = \begin{bmatrix} A_0 & \cos(\omega_n t_i) & \sin(\omega_n t_i) \\ \vdots & \vdots & \vdots \\ A_0 & \cos(\omega_n t_i) & \sin(\omega_n t_i) \end{bmatrix}$$

Then, an observation matrix (F) is created containing water surface height data at time intervals that meet temporal sampling requirements. The observation equation is formulated as follows:

$$h(t) = Z_0 + \sum_{i=1}^{n} A_n cos(\omega_n\, t_i) - \sum_{i=1}^{n} B_n sin(\omega_n\, t_i)$$

Next, a parameter matrix (X) is formed through multiplication between matrix A and matrix F. This parameter matrix produces the average water surface constant value (Z_0), as well as amplitude coefficients (A_i) and phase coefficients (B_i) of each component. From these parameters, the amplitude and phase of each component can be calculated mathematically.

$$[X] = (ATA)^{-1}A^T L$$

$$[\mathrm{X}] = \begin{bmatrix} Z_0 \\ A_i \\ B_i \end{bmatrix}$$

The tidal constants used in this study are determined based on frequency limitations, namely Sa and Ssa components, with predetermined angular velocity values. With these parameters, a mathematical model of tidal phenomena is built using the equation:

$$\boldsymbol{h(t_i) = A_0 + \sum_{i=1}^{n} amp_i \cos(\omega_i t_i - \emptyset_i)}$$

The quality of the resulting analysis model is then tested by calculating the Pearson correlation coefficient between observational data and model results. This test aims to determine the strength and direction of linear relationships between satellite-recorded tidal data and the constructed harmonic model.

Results and Discussion

An overview of water levels at Lake Toba based on ICESat-2 ATL-13 data is presented in Figure 2.

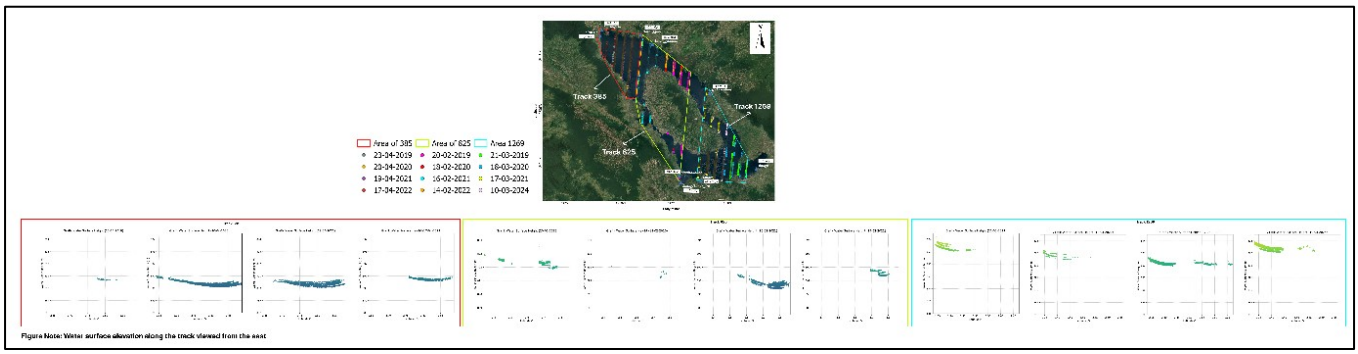

Souce: Personal Documentation

Figure 3: Water Level Profile of Lake Toba

Based on Figure 3, water levels in the eastern part (Track 1269) of Lake Toba have higher water levels compared to the western (Track 385) and central (Track 825) parts. The average water level of each track can be seen in Table 3.

Table 3: Average Water Level of Each Track

Track	WSH Average (m)
385	890.55
825	891.496
1269	892.953

As shown in Table 3, it appears that water levels in the western zone of Lake Toba have the lowest water level compared to central and eastern zones. This may be due to the possibility of river inlets with small inlet discharge, such as Sipiso-piso River, Sitio-tio River, Haranggaol River which have water discharge of ±0.2 m^3/second (Lukman, 2013). Meanwhile, water levels in the eastern zone of Lake Toba have the highest elevation, possibly due to river inlets with large discharge, such as Silang River (±10 m^3/second), Naborsahan River (±2 m^3/second), Halian River (±2 m^3/second), and Sipultakhuda River (±1.4 m^3/second), thus contributing to increased lake water volume in that area, resulting in relatively higher water levels compared to other zones. River inlets are just one factor causing water level differences in lakes. Further integrated studies with data such as meteorological conditions, topographic conditions, land use, and geological and soil substrate conditions (Manurung et al., 2015) are needed to obtain absolute conclusions regarding water level differences in Lake Toba zones.

In the central zone of Lake Toba, there is Samosir Island in the middle. The presence of land, vegetation, and water edge features (land cover) affects ground track data collection from ATL13. The aspect that appears quite clear is fewer ground tracks passing through compared to other tracks because ATL13 works by detecting only waters, including lakes, reservoirs, rivers, bays, estuaries, and coastal buffer areas along 7 km (Jasinski et al., 2023).

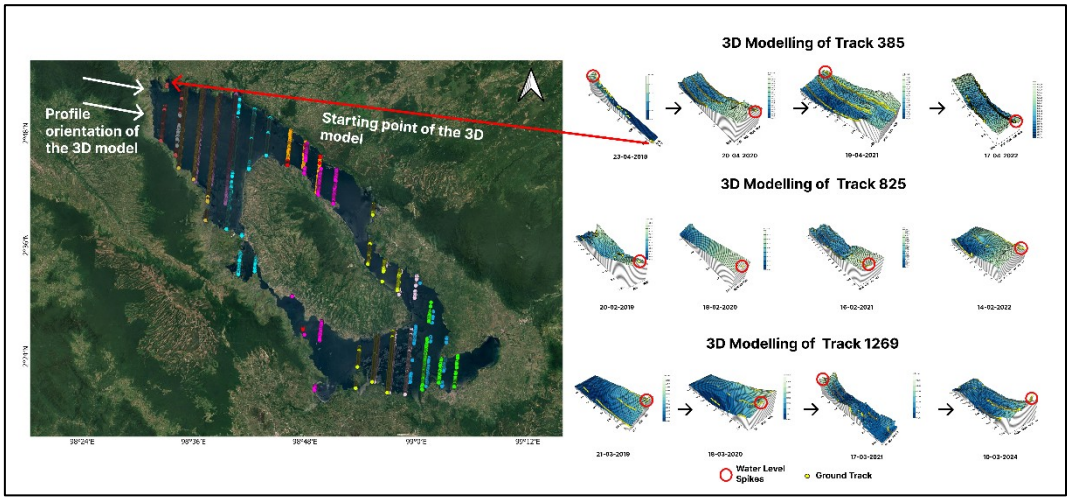

Souce: Personal Documentation

Figure 4: Spatial Distribution of the 3D Model for Each Track

Figure 4 presents a three-dimensional model for water levels on each date with a view from northwest of Lake Toba, with the three-dimensional model reading direction starting from the north. Based on ICESat-2 data passing through Lake Toba, there is a phenomenon of water level spikes toward land indicated by red circles in Figure 4. Seiche is a standing wave that oscillates in a water body, similar to water swaying back and forth in a pool after being shaken (NOAA, 2024). Seiche causes the water surface to appear to rise on one side and fall on the other side; this phenomenon is found at lake edges. Based on this explanation, the pattern depicted in Figure 3 can be an initial indication that the spike pattern occurring at Lake Toba is a seiche phenomenon. However, supporting data such as meteorological data is needed to produce absolute conclusions.

Research by Monahan et al (2025) showed that a satellite called Surface Water and Ocean Topography (SWOT) successfully proved seiche phenomena in fjords using satellite altimetry for the first time. This phenomenon could be captured due to SWOT's high spatial resolution. Through similar principles, ICESat-2 has great potential to detect seiche phenomena. However, due to quite long temporal resolution of 91 days, the full oscillation phase of seiche will be difficult to capture. Additionally, available data on ICESat-2 is in track form, making it difficult to see potential two-dimensional oscillations on the water surface. To produce similar

conclusions, ICESat-2 data needs to be combined with other supporting data such as seismic or meteorological data to produce conclusions about the presence or absence of seiche phenomena at Lake Toba.Water levels at Lake Toba on Tracks 385, 1269, and 825 can be seen in Table 3.

Table 3: Water Surface Elevation and Fluctuations for Each Track

Track	Date	WSH Average (m)	Flucktuation (m)
385	23/04/2019	890,719	-0,311
	20/04/2020	890,408	
	19/04/2021	890,350	-0,058
	17/04/2022	890.723	0,373
1269	21/03/2019	893,377	-0,510
	18/03/2020	892,867	
	17/03/2021	892,198	-0,669
	10/03/2024	893,370	1,172
825	20/02/2019	892,259	-0,822
	18/02/2020	891,437	
	16/02/2021	890,748	-0,689
	14/02/2022	891,538	0,790

Based on Table 3, it can be seen that at Lake Toba, water level decline occurred from 2020 to 2021 with ranges between 0.058 to 0.689 meters. The water level decline in 2021 was reported

by Sinaga & Warastri (2021), on April 7, 2021, that low water levels can be influenced by several factors. The first possibility is that rainwater is still filling groundwater that has dried up. Another possibility is that the outgoing water used for hydroelectric power plants is still greater than the rainwater entering Lake Toba's catchment area. This becomes crucial because it can hinder hydroelectric power plant and pier activities. Nevertheless, the contribution of each factor needs further study through integrated hydrological approaches.

Water level trends began to improve after 2022 until 2024. This phenomenon possibly occurred due to rainfall spikes recorded due to the La Niña effect that occurred from mid-2020 to the end of 2022. La Niña 2020-2021 had a moderate index with increased monthly rainfall (Hatif, 2021). Nevertheless, there was a water level decline trend in 2021 because La Niña only occurred in 2020, so in early 2021 the rainy season had not significantly influenced yet, and rainfall only increased 20%-70% in October 2021 (Hatif, 2021). Manurung (2024) revealed in news published on March 21, 2024, that this water surface rise was caused by increased underground water discharge after the rainy season, so more rainwater entered the soil rather than falling into Lake Toba. This statement aligns with the fact of water level rise in 2022 and 2024, so the possibility of water level rise at Lake Toba is due to additional underground water supply. Nevertheless, the relationship between groundwater and water levels at Lake Toba is a complex relationship, requiring further validation through integrated hydrological studies.

To determine periodic properties in sample areas of Track 385, Track 825, and Track 1269 at Lake Toba, harmonic analysis was used by testing Sa and Ssa constants because both constants meet frequency limits. The measure of strength and direction of data linearity relationship with its model will be tested using the Pearson formula (r). The correlation results and coefficients are presented in Table 4.

Table 4: Correlation Coefficient Test Results for Each Track

Track	r	Correlation
385	0.824	Strong
1269	0.813	Strong
825	0.625	Moderate

Sa and Ssa waves detected will be examined for their wave energy through amplitude magnitude in Sa and Ssa waves. The wave energy magnitude that influences water level dynamics occurring in Tracks 385, 1269, and 825 is presented in Table 5.

Table 5: Sa and Ssa amplitudes for each track

Track	Sa (m)	Ssa (m)
385	2.781	1.608
1269	0.441	0.541
825	0.072	1.524

Through wave energy percentage information on Track 385, the Sa constant gives 63.36% results and the Ssa constant gives 36.64% results. The Sa constant becomes the dominant energy forming water level dynamics, while Ssa does not significantly influence. The Sa component has an annual period, so its contribution will be felt seasonally in a one-year cycle influenced by the sun's position relative to earth during one year.

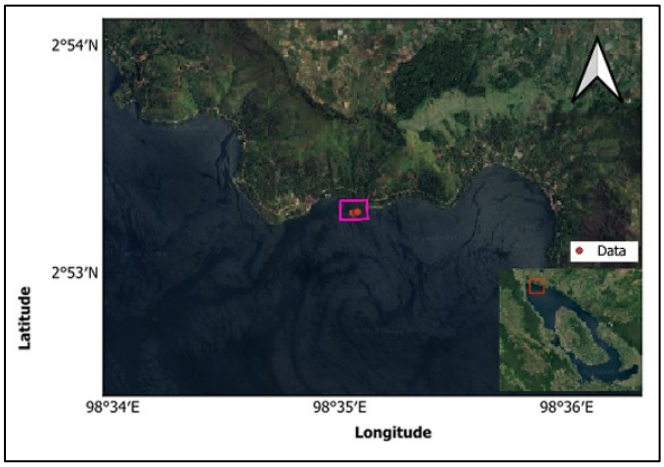

Souce: Personal Documentation

Figure 5: Sample Area with 45 m × 45 m Boundaries

When spatial data size is reduced as in Figure 5, 4 samples with close positions are obtained, bounded by a 45 m × 45 m area, as in Figure 5 with different sample dates, the resulting dominant waves become different. The Pearson formula test and amplitude are presented in Table 6.

Table 4: Results of Pearson Test and Amplitude in a Small Area of Track 385

Component	r	Correlation	Amplitude (m)
Sa	0,88	Strong	0.2802
Ssa	0.65	Moderate	1.001

Through wave energy percentage information on Track 385 with smaller spatial area samples, the Sa constant gives 21.88% results and the Ssa constant gives 78.12% results. The Ssa constant becomes the dominant energy forming water level dynamics, which is opposite to the calculation results using Table 4. Although Sa has strong correlation, the energy produced by Ssa forms waves in that area.

Although sample data locations are near land, where spatially Sa will tend to be stronger near land due to various local phenomena such as wind variations, temperature, salinity, and local hydrology (Vinogradov & Ponte, 2010), processing results show Ssa dominates energetically. Through this fact, it can be indicated that local phenomena occurring will depend on the size of the studied area.

When area coverage is reduced, detection of energy fluctuations influenced by local phenomena becomes more visible, so areas with high spatial resolution can identify local influences in more detail. This explanation becomes relevant because Ssa waves dominate in smaller areas. If Ssa dominates, water level fluctuations can occur by following seasons that form semi-annual atmospheric patterns every 6 months, supported by atmospheric studies showing air temperature and pressure patterns that also change semi-annually (Shangguan & Wang, 2022).

This is then strengthened through research by Yulihastin & Kodama (2014), namely the Medan region shows a semiannual oscillation pattern. Although there is no explicit classification for Lake Toba, its geographical position close to Medan allows semi-annual atmospheric influences to play a role in water level fluctuations. Semiannual oscillation (SAO) is a component of the annual cycle of a variable consisting of sinusoidal oscillations with a six-month period. This component can affect seasonal rainfall patterns, temperature and atmospheric pressure changes, and water level fluctuations aligned with semi-annual tidal waves. This opens the possibility that semi-annual seasonal changes in temperature and rainfall also affect water level fluctuations at Lake Toba, especially in Ssa wave formation.

In the energy percentage calculation results, on Track 825, the Sa constant gives 5% results and the Ssa constant gives 95% results. The Ssa constant becomes the dominant energy forming water level dynamics. The Ssa component occurs due to semi-annual variation with a 183-day period, having 2 rise-fall periods per year.

Although Sa and Ssa correlation coefficients produce strength of 0.625, which is moderate, detrending cannot be performed because it would produce an overfitting model since the components used would exceed available data, resulting in extreme correlations and coefficients and predictions that do not represent real conditions (Hastie et al., 2017) Detrending is the process of removing trends from time series data to ensure data stationarity.

On Track 1269, the Sa constant gives 44.92% results, while Ssa gives 55.08%. The Ssa constant becomes the dominant energy forming water level dynamics compared to Sa. The Ssa component occurs due to semi-annual variation with a 183-day period, having 2 rise-fall periods per year. There are quite extreme water level decline and spike phenomena on Track 1269, with visualization of these phenomena presented in Figure 6.

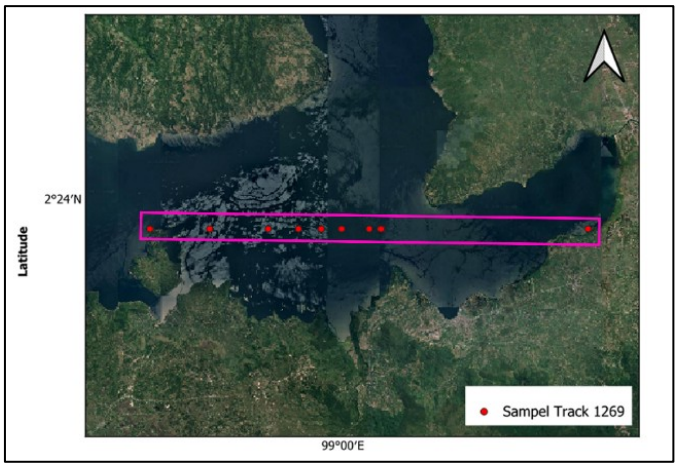

Souce: Pers

onal Documentation

Figure 6: Area Bondaries for Track 1269

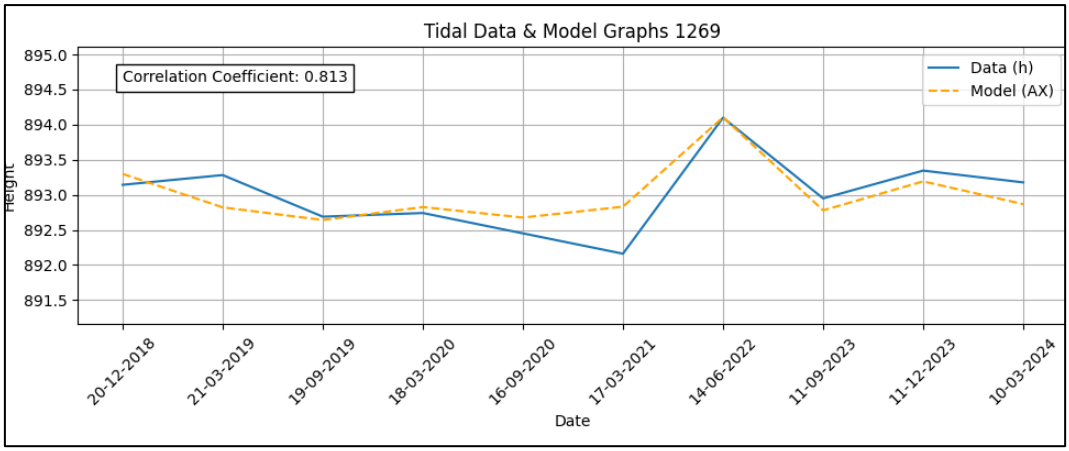

Souce: Personal Documentation

Figure 7: Temporal Variation of Water Level in the Sample Area of Track 1269

In Figure 7, the lowest water level is on March 17, 2021, with a value of 892.161 meters. The indication of factors causing this drastic water level decline is due to rainfall at Lake Toba classified as low to moderate and rain characteristics below normal in March 2021 (BMKG, 2021).

There is a water level spike on June 14, 2022, which is the highest water level as seen in Figure 6, at 894.099 m. This phenomenon becomes the largest spike due to rainfall at Lake Toba classified as above normal (Prasetyaningtyas, 2022). This phenomenon is caused by the La Niña effect that occurred from mid-2020 to the end of 2022 (Ibrahim, 2022). This phenomenon caused many areas that should have been dry in June to be drenched by heavy rain until mid-June (Hanan, 2022). This condition shows that global climate variability, such as La Niña, has real influence on Lake Toba water level fluctuations, so it needs to be considered in long-term analysis. The dominant Ssa component amplitude energy on Track 1269 also reached its peak in June, considering the Ssa component cycle that repeats every half year. This also adds factors to the spike that occurred in June.

Water surface anomalies like La Niña can be successfully captured clearly using ICESat-2 during La Niña 2019 and Indian Ocean Dipole 2019 using ATL12 data products (Buzzanga et al., 2021). This phenomenon can be captured due to ICESat-2's high spatial resolution, enabling it to show sea level rise phenomena and even capture small features like currents and eddies. With this capability, collaborative data between ATL12 and ATL13 from ICESat-2 has potential in monitoring lake water level dynamics, particularly in identifying hydrological responses to climate phenomena like La Niña.

Conclusion and Recommendation

Based on analysis of ICESat-2 Track 385, Track 825, and Track 1269 data at Lake Toba, it was found that water levels at Lake Toba in the eastern zone are higher than western and central zones with differences reaching ±2.4 meters; there is a pattern of water accumulation toward land in the three-dimensional water level profile; between 2018 to 2024, the lowest water level at Lake Toba occurred in 2021; and generally, water level change patterns are influenced by annual (Sa) and semi-annual (Ssa) cycles with Ssa being more dominant.

The recommendations that can be given after conducting this research are: Longer observation data is needed to obtain diverse water level change pattern characteristics; In subsequent research, meteorological data can be added to strengthen indications of seiche phenomena at Lake Toba; Future research can use ATL-12 data to understand the impact of climatological factors on ocean water levels; and ICESat-2 ATL13 data can be used by the National Priority Lake Rescue Team to monitor water levels of 15 National Priority Lakes as information for further planning and development of priority lakes.

References

Budianto, Y. (2023, June 16). *Menyusutnya Separuh Cadangan Air Tawar Danau di Dunia*. In Kompas.com. Retrieved February 24, 2025 Kompas. https://www.kompas.id/artikel/menyusutnya-separuh-cadangan-air-tawar-danau-di-dunia

De Wit, M., & Stankiewicz, J. (2006). Changes in surface water supply across Africa with predicted climate change. *Science*, *311*(5769), 1971–1921. https://doi.org/10.1126/science.1119929

Fernando, G., & Pedro, G. (2023). Estimating the Water Level and Bathymetry of Lake Yahuarcocha, Ecuador Using ICESat-2/ATL13 Satellite Laser Altimetry, System Dynamics Model, and Machine Learning. *Communications in Computer and Information Science*, *1781 CCIS*, 98–111. https://doi.org/10.1007/978-3-031-35641-4_7

Hanan, A. (2022, June 10). *Juni Masih Hujan? Ini Penjelasan dari BMKG. In* nu.or.id. Retrieved June 7, 2025, from https://www.nu.or.id/nasional/juni-masih-hujan-ini-penjelasan-dari-bmkg-HyPhM

Hastie, T., Tibshirani, R., & Friedman, J. (2017). *The Elements of Statistical Learning: Data Mining, Inference, and Prediction*. Springer.

Hatif, T. (2021, October 18). *BMKG: Waspada La Nina dan Peningkatan Risiko Bencana Hidrometerologi*. In bmkg.go.id. Retrieved July 15, 2025, from https://www.bmkg.go.id/siaran-pers/bmkg-waspada-la-nina-dan-peningkatan-risiko-bencana-hidrometerologi

Hidayat, A. (2020, February 4). *PLTA Hasang Beroperasi, PLN Tambah Pemanfaatan Pembangkit EBT*. In web.pln.co.id. Retrieved May 5, 2025, from https://web.pln.co.id/cms/media/siaran-pers/2020/02/plta-hasang-beroperasi-pln-tambah-pemanfaatan-pembangkit-ebt/

Ibrahim. (2022). *BMKG: Fenomena La Nina Triple Dip Jadi Ancaman Negara-negara di Dunia*. In bmkg.go.id. Retrieved June 7, 2025, from https://www.bmkg.go.id/siaran-pers/bmkg-fenomena-la-nina-triple-dip-jadi-ancaman-negara-negara-di-dunia

Jasinski, M., Gsfc, N., Stoll, J., Hancock, D., Robbins, J., Nattala, J., Morison, J., Jones, B., Ondrusek, M., Parrish, C., Ssai, C. C., Jasinski, M., Stoll, J., Hancock, D., Robbins, J., Nattala, J., Morison, J., Jones, B., Ondrusek, M., … Carabajal, C. (2023). *ICESat-2 Algorithm Theoretical Basis Document (ATBD) for Along Track Inland Surface Water Data, ATL13, Version 6*. https://doi.org/10.5067/03JYGZ0758UL

Liu, C., Hu, R., Wang, Y., Lin, H., Zeng, H., Wu, D., Liu, Z., Dai, Y., Song, X., & Shao, C. (2022). Monitoring water level and volume changes of lakes and reservoirs in the Yellow River Basin using ICESat-2 laser altimetry and Google Earth Engine. *Journal of Hydro-Environment Research*, *44*, 53–64. https://doi.org/10.1016/J.JHER.2022.07.005

Manurung, P. (2024, March 21). *Ahli Geologi Ungkap Fakta Air Danau Toba Naik Hingga 2 Meter Tiap Tahun*. Mistar. In mistar.id. Retrieved May 7, 2025, from https://mistar.id/news/simalungun/ahli-geologi-ungkap-fakta-air-danau-toba-naik-hingga-2-meter-tiap-tahun

Manurung, P., Gaol, J. L., Katarina, F., & Ketaren, D. (2015). Kondisi Aktual Danau Toba: Pemantauan Real Time Tinggi Permukaan Air Dan Kajian Sustainabiliti Danau Toba . *Seminar Dan Pameran—Save Lake Toba*.

Monahan, T., Tang, T., Roberts, S., & Adcock, T. A. A. (2025). Observations of the seiche that shook the world. *Nature Communications*, *16*(1), 4777. https://doi.org/10.1038/s41467-025-59851-7

Phan, V. H., Lindenbergh, R., & Menenti, M. (2012). ICESat derived elevation changes of Tibetan lakes between 2003 and 2009. *International Journal of Applied Earth Observation and Geoinformation*, *17*(1), 12–22. https://doi.org/10.1016/J.JAG.2011.09.015

Prasetyaningtyas, K. (2022). *Analisis Curah Hujan dan Sifat Hujan Juni 2022*. In bmkg.go.id. Retrieved June 7, 2025, from https://www.bmkg.go.id/iklim/analisis-curah-hujan-dan-sifat-hujan-juni-2022

Rini, C. L. (2022, April 22). Danau Toba, Penggerak PLTA dan Smelter Inalum. In republika.id. Retrieved February 24, 2025, from https://www.republika.id/posts/26659/danau-toba-penggerak-plta-dan-smelter-inalum

Robertson, D., & Ragotzkie, R. (1990). Changes in the thermal structure of moderate to large sized lakes in response to changes in air temperature. *Aquat Sci*, *52*, 360–380. https://doi.org/https://doi.org/10.1007/BF00879763

Rosid, M. S., Irwandi, H., Apip, Mart, T., Susanto, R. D., & Sulaiman, A. (2025). Evaluation of Lake Toba's water level decline in Indonesia over the past six decades. *Environmental Challenges*, *18*. https://doi.org/10.1016/j.envc.2024.101071

Shangguan, M., & Wang, W. (2022). The semi-annual oscillation (SAO) in the upper troposphere and lower stratosphere (UTLS). *Atmospheric Chemistry and Physics*, *22*(14), 9499–9511. https://doi.org/10.5194/acp-22-9499-2022

Sichangi, A. W., Wang, L., Yang, K., Chen, D., Wang, Z., Li, X., Zhou, J., Liu, W., & Kuria, D. (2016). Estimating continental river basin discharges using multiple remote sensing data sets. *Remote Sensing of Environment*, *179*, 36–53. https://doi.org/10.1016/J.RSE.2016.03.019

Sinaga, N., & Warastri, A. W. (2021, April 7). *Tinggi Muka Air Danau Toba Menurun Drastis, Modifikasi Cuaca Dilakukan*. In kompas.id. Retrieved March 3, 2025, from https://www.kompas.id/artikel/tinggi-muka-air-danau-toba-menurun-drastis-modifikasi-cuaca-dilakukan

Thesalonika, E. (2017). *Danau Toba Dalam Perspektif Historis Menuju Destinasi Wisata Dunia* [Skripsi]. Universitas Negeri Medan.

Vinogradov, S. V., & Ponte, R. M. (2010). Annual cycle in coastal sea level from tide gauges and altimetry. *Journal of Geophysical Research: Oceans*, *115*(C4). https://doi.org/10.1029/2009JC005767

Xiang, J., Li, H., Zhao, J., Cai, X., & Li, P. (2021). Inland water level measurement from spaceborne laser altimetry: Validation and comparison of three missions over the Great Lakes and lower Mississippi River. *Journal of Hydrology*, *597*. https://doi.org/10.1016/j.jhydrol.2021.126312